

MULTI-OBJECTIVE OPTIMIZATION OF 3D BEAM TRACKING IN ELECTROSTATIC BEAMLINES*

V. Rodin[†], J. Resta-Lopez, J. R. Hunt, B. Veglia, C. P. Welsch,
University of Liverpool, UK and The Cockcroft Institute, Daresbury, UK

Abstract

After CERN's Long Shutdown 2 (LS2) the Extra Low Energy Antiproton (ELENA) ring will begin transporting extremely low energy (100 keV) antiproton beams to the antimatter experiments. To provide simultaneous operation and obtain the greatest efficiency, transfer lines will be based on electrostatic optics and short pulse (~ 100 ns) deflection. Unfortunately, only a small number of simulation codes allow realistic and flexible implementation of such elements limiting our prediction capabilities of beam behaviour.

In this contribution, methods for accurately modelling and tracking through electrostatic optical elements are presented, utilising a combination of finite element methods or experimental measurements with both a modified version of G4Beamline and BMAD. Multi-objective optimization techniques are used in order to achieve desirable lattice parameters and beam quality at various points along the transfer lines. Realistic beam distributions obtained via tracking around ELENA in the presence of collective effects and electron cooling are propagated along the optimized 3D transfer lines models.

INTRODUCTION

Considering possible errors associated with machine elements is important during the design and construction of all accelerator systems. Linear machine, synchrotron or transfer line transmission efficiency might be decreased by intrinsic machine instabilities like the non-uniform field shape of the magnetic or electrostatic optical elements. Another issue could be the time dependence of the applied field in fast deflectors. These effects become more relevant in non-relativistic cases like the study of extra low energy (< 100 keV) antimatter physics [1,2] or in the fields of low energy (\approx MeV/a.m.u) nuclear and atomic physics [3], limiting beam intensity and compromising expected quality.

The major effort of this study is the extension of capabilities of existing tools and development of new methods for fast but realistic and thorough particle tracking simulations combined with comprehensive optimization techniques. Here we show such an implementation of the electrostatic transfer line from ELENA to the ALPHA experiment [4] since we may compare our new methods against pre-existing simulations. Subsequently, it will help to determine and match beam parameters at the experiment, and eventually benchmark simulation results with real measurements of beamlines which will become operational after the LS2.

For such low energy particles, even small electrostatic field imperfections may lead to a significant change of the orbit and expansion of the beam profile. Hence, the simulation techniques should take into account many combined factors including parameterized shapes of inhomogeneous and fringe fields, stray magnetic fields, residual gasses, real geometry of electrodes, space charge effects and other additional scattering and collective effects. In order to compensate for negative impacts, multi-objective optimization may be applied.

BEAM TRACKING TOOLS

For the investigation into the beam dynamics of the transfer lines, two main programs were used. One of them is G4Beamline code [5], a Geant4 based project that allows a user to modify various parameters of provided functionality. Software flexibility and simplicity make it a very robust tool on which we base on our primary studies. Another advantage is a simple approach in the implementation of electric or combined electro-magnetic fields. Additionally, these fields can be varied in time which gives a user the possibility to construct complicated structures such as united storage rings and transfer lines.

The Geant4 based simulation propagates a user-generated 6D beam distribution through the voxelized 3D world taking into account the aspects changing particle movement and exploiting the impact of the defined physics processes at each step. Primarily, the main source of constraints in the beam transfer line is EM fields. The differential equation of motion of the particle is solved for propagation inside quadrupole or dipole field distributions. By default, this is performed using the so-called Dormand-Prince 5th order integration method [6] which is commonly used for differential system solving. However, due to its stepping nature, it usually introduces a small error ($\sim 10^{-5}\%$) which can be mitigated even further by decreasing step of integration. In addition, numerous physical models or experimentally based physics lists can be applied to accurately simulate non-relativistic energy hadron behaviour [7].

Another tool that was chosen for benchmarking studies is BMAD [8], a Fortran based subroutine library for relativistic charged particle simulations in high energy accelerators and storage rings. Therefore, some low energy effects are not taken into account. It contains different tracking algorithms including Runge-Kutta and symplectic field integration. As opposed to particle tracking codes such as MAD-X [9], combined function lattice elements can be used. BMAD supports a list of algorithms for a nonlinear optimization for finding the local minimum (or maximum) of the defined function.

* Work supported by EU Horizon 2020 research and innovation programme under the Marie Skłodowska-Curie grant agreement No 721559.

[†] volodymyr.rodin@liverpool.ac.uk

TRANSFER LINE ELEMENTS

G4Beamline includes a set of predefined magnetic elements and different functions permitting the user to save all needed tracking information. However, as mentioned previously, the ELENA transfer lines are electrostatic. Therefore, in order to describe actual electrostatic optics a G4Beamline modification was made [10]. The shape and intensity of the quadrupole field are based on experimental field measurements [11] and implemented in the simulation utilising Enge function [12] coefficients, Fig. 1.

Due to a complex design and in order to include fringe regions, electrostatic beamline deflectors were replaced by the field maps generated in CST [13], Fig. 2. Also to make the field map aligning procedure easier, the actual element geometry was imported. This import functionality can also be used to simulate the complex geometry of degrading targets on ALPHA experiment if needed.

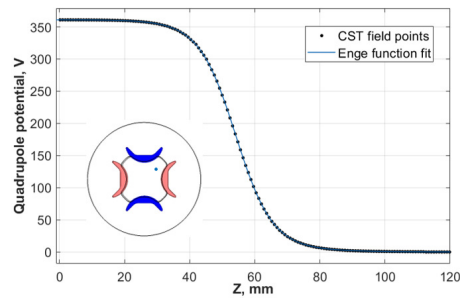


Figure 1: Enge function fit of quadrupole potential axis for ± 811 V applied on electrodes. The blue dot on the section plane represents the position of voltage evaluation line.

Benchmarking and analytical analysis of field maps were performed in BMAD. The field map defines the field in the transverse (x, y) plane at constant z in local cartesian, cylindrical or centerline coordinates and can be anchored to fields containing elements such as quadrupoles, bends and cavities. However, the that usual field output from CST or Opera consists of a combination of bending element and drifts for the fringe regions thus field maps used in G4Beamline must be divided into three different sections: drift before bending, bending element and drift after bending, Fig. 3. Separate coordinate system transformations for each component according to the centerline are also required.

GENERATION OF BEAM DISTRIBUTION

The beam in accelerator physics can be represented as a 6D distribution of particles. The six dimensions are three canonical conjugate coordinate pairs in three planes, and can be described by the vector: $\mathbf{u} = (x, x', y, y', \tau, \delta)$. The mean values of that distribution are the beam centroids. The 6x6 matrix of second order moments of the distribution or shortly $\mathbf{U}_{ij} = \langle x_i x_j \rangle$ is referred to as sigma values for multi-dimensional Gaussian beam where the angle brackets denote a central moment. Also the beam is typically parametrised in an accelerator using the Twiss functions β, α, γ and dispersions $\eta_x, \eta_{x'}, \eta_y, \eta_{y'}$. These are used in combination with

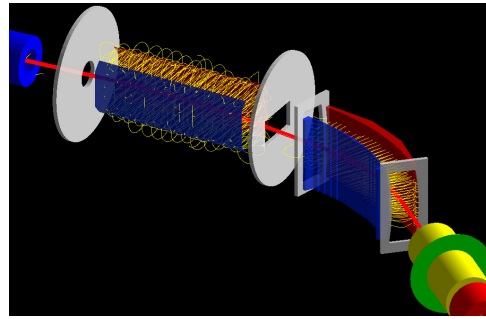


Figure 2: Combination of two bends with CAD geometry in G4Beamline. Electrodes are colored according applied polarity, assuming a negatively charged beam (red). Yellow lines are computed field lines based on the field map values.

beam transverse emittances ϵ_x, ϵ_y and longitudinal parameters $\sigma_\delta, \sigma_\tau$. The combination of machine and beam parameters gives the physical observables such as beam size [14].

Because of the dispersion and energy spread present in the real beam, longitudinal-transverse and transverse-transverse couplings were introduced, which are defined as off-diagonal elements in the sigma matrix. To ensure that we have a positive variance in each dimension, the \mathbf{U}_{ij} matrix must be positive definite. To obtain each term of the covariance matrix, we consider the effect of dispersion on single coordinates. For example, for an individual particle, the horizontal position is affected as follows: $x_i = x_{\beta i} + \eta_s \delta_i$, where x_i is the horizontal transverse coordinate, $x_{\beta i}$ is the betatron component and $\eta_s \delta_i$ reflects the change due to the particle's relative energy offset in a dispersive region.

Due to independency and the random nature of $x_{\beta i}$ and δ_i , the second order moment in x_β can derived from the properties of the variance: $\langle x^2 \rangle = \epsilon_x \beta_x + \eta_x^2 \sigma_\delta^2$, obtained by applying the Courant-Snyder equations and rewriting the variance in terms of standard deviation. An interrelationship

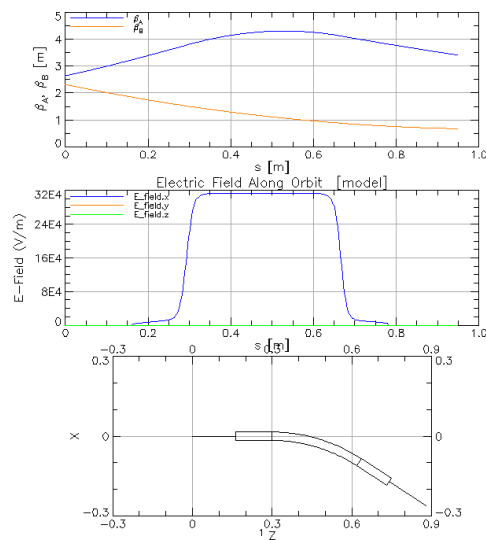


Figure 3: Electrostatic bending element divided in three parts (bottom) with its corresponding electric field (middle) and $\beta_{x,y}$ function evolution (top).

Content from this work may be used under the terms of the CC BY 3.0 licence (© 2019).

that involves two different variables affected by dispersion has the same form. For example:

$$\langle x x' \rangle = \langle x_\beta x'_\beta \rangle + \eta_x \eta_{x'} \langle \delta^2 \rangle = -\epsilon_x \alpha_x + \eta_x \eta_{x'} \sigma_\delta^2 \quad (1)$$

All other couplings can be done in the same manner.

Reverse Analysis

In the previous section it was mentioned that an ensemble of particles can be characterised by Twiss functions which is the simple way to analyse beam evolution along the transfer line. Because G4Beamline describes each particle using x, y, z coordinates in mm and 3 momentum components (P_x, P_y, P_z) in MeV/c a reverse calculation of Twiss variables for every propagation step was performed using the statistical definition of emittance:

$$\epsilon_{x,rms} = \sqrt{\langle x^2 \rangle \langle (x')^2 \rangle - \langle x x' \rangle^2} \quad (2)$$

MULTI-OBJECTIVE OPTIMIZATION

In order to maximize transmission and obtain various desired characteristics, the real beamline must be tuned. To determine the parameters of beamline elements (e.g. length, optical strength), conventional beam dynamics programs can be used. On the other hand, due to simplifications and ignoring many side effects that G4Beamline implements, these programs give approximated values. G4Beamline provides basic tuning of the lattice via *tune* command, where only chosen elements can be optimized. These include dipoles, field maps and cavities that can be optimized by a number of iterations, solving a single-objective problem with one parameter.

An extra tuning of quadrupoles can be performed by external program packaged together with G4Beamline [15] based on MINUIT library that minimizes the value of the given function in single point, like multiple FODO cell focusing. So to fill the gap, an additional multi-objective optimization algorithm was utilised. The common technique to solve such types of problem is nondominated sorting genetic algorithm II (NSGA-II) [16] but due to the high number of evaluations for the meaningful result, another method was chosen.

Paretosearch is a new multi-objective algorithm added in the recent version of Matlab (R2018b) [17]. One of the main advantages of *paretosearch* is that it usually takes many fewer function evaluations and typically when the problem has no nonlinear constraints, *paretosearch* is at least as accurate as NSGA-II [18].

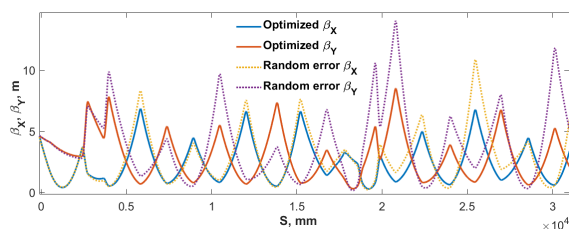


Figure 4: The transfer line optics before and after tuning.

To study the efficiency of this algorithm a quadrupole strength error of up to 10 % in comparison with design values was randomly introduced into the beamline. As the set of objectives a minimization of peak values of β_x and β_y whose amplitude is above 8 m and zero losses along the transfer line was requested. After around a hundred evaluations these conditions were satisfied, Fig. 4.

CONCLUSIONS AND OUTLOOK

At the present moment, we fully understand the method which will fully describe any transfer line using the realistic description of elements and the injected beam. External benchmarking in BMAD using a fully analytical approach is possible and can be used for studying long time processes in storage rings.

The new features were added to G4Beamline to make the simulation process more versatile. The transverse and longitudinal beam definition by Twiss functions allowed to investigate more properties of the lattice such as bunch length compression, Fig. 5. Finally, the convenient multi-objective optimization technique helps to fix problems caused by element approximations or tune the lattice to desired outcome.

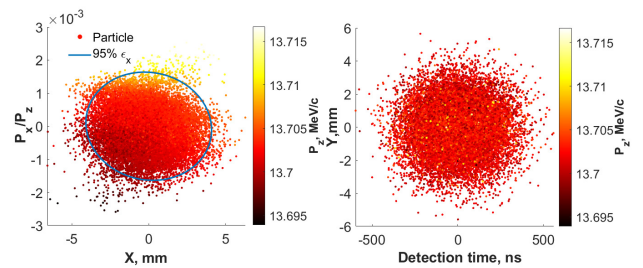


Figure 5: Beam profile at the end of the line. The blue ellipse (left) represents scaled ϵ_x . Right plot shows arrival times of particles assuming 0 ns time for the reference momentum particle. An initial bunch length was preserved and has $\sigma_\tau=150$ ns.

Future aims include expansion of the model to other experiments. The impact of stray fields on the performance of the current beamline will be investigated. Additionally, the multi-objective optimization will be added to the existing version of the GUI interface [19]. Finally, *tune* command can be improved to optimize Twiss functions as well.

ACKNOWLEDGEMENTS

We greatly appreciate for the helpful input of our friends and colleagues at CERN. Also, we extend thanks for the fruitful discussions with code developers David Sagan, Tom Roberts and Geant4 forum users.

REFERENCES

- [1] V. Chohan et al., (Ed.), "Extra Low Energy Antiproton ring (ELENA) and its Transfer Lines", Design Report, CERN-2014-002, 2014.

Content from this work may be used under the terms of the CC BY 3.0 licence (© 2019). Any distribution of this work must maintain attribution to the author(s), title of the work, publisher, and DOI

- [2] E. Widmann, "Low-energy antiprotons physics and the FLAIR facility", *Phys. Scr.*, vol. 2015, no. T166, pp. 014074, Nov. 2015.
- [3] Y. Kadi, "HIE-ISOLDE : technical design report for the energy upgrade", CERN Yellow Reports: Monographs, CERN, 2018.
- [4] M. Ahmadi *et al.*, "Observation of the 1S–2S transition in trapped antihydrogen", *Nature*, vol. 541, pp. 506-510, Jan. 2017.
- [5] T. J. Roberts and D. M. Kaplan, "G4beamline simulation program for matter-dominated beamlines", in *Proc. 22nd Particle Accelerator Conf. (PAC'07)*, Albuquerque, USA, June 2007, paper THPAN103, pp. 3468–3470.
- [6] J. R. Dormand, P. J. Prince, "A family of embedded Runge-Kutta formulae", *Journal of Computational and Applied Mathematics*, pp. 19–26, 1980.
- [7] S. Chauvie *et al.*, "Geant4 model for the stopping power of low energy negatively charged hadrons", *IEEE*, vol. 54, no. 3, pp. 578–584, Jun. 2017.
- [8] D. Sagan, "Bmad: A relativistic charged particle simulation library", *Nuclear Instruments and Methods in Physics Research A*, 558, 2006.
- [9] MAD - Methodical Accelerator Design, <http://mad.web.cern.ch/mad/>.
- [10] V. Rodin *et al.*, "Realistic 3D implementation of electrostatic elements for low energy machines", *Hyperfine Interact* 240: 35, 2019.
- [11] Andreas Kainz *et al.*, "Non-invasive 3D field mapping of complex static electric fields", submitted to *Phys. Rev. Lett.*
- [12] H.A. Enge, "Deflecting magnets", in A. Septier (ed.) *Focusing of charged particles*, Vol. 2, Academic Press, pp. 203–264, 1967.
- [13] CST Studio Suite, <https://www.cst.com/products/csts2/>.
- [14] J. R. Hunt *et al.*, "Emittance measurements in low energy ion storage rings", *Nucl. Instr. Meth.*, Volume 896, pp 139-151, 2018.
- [15] Muons, Inc - gminuit, <http://www.muonsinternal.com/muons3/gminuit/>.
- [16] K. Deb, "A fast and elitist multiobjective genetic algorithm: NSGA-II", *IEEE Transactions on Evolutionary Computation*, pp 182-197, Aug. 2002.
- [17] A. L. Custódio *et al.*, "Direct Multisearch for Multiobjective Optimization", *SIAM J. Optim.*, pp. 1109–1140, 2011.
- [18] Multi-objective optimization comparison, <https://uk.mathworks.com/help/gads/multiobjective-optimization-welded-beam.html>.
- [19] J. R. Hunt *et al.*, "3D Tracking Methods in a GEANT4 Environment Through Electrostatic Beamlines", in *Proc. IPAC'18*, Vancouver, Canada, April-May 2018, paper THPAF016, pp. 2979-2982.